Detailed Methods

Animal Use

All procedures were approved by and conducted in accordance with The University of Texas at Austin Institutional Animal Care and Use Committee. Male and female Mongolian gerbils (*Meriones unguiculatus*) were bred at the Animal Resource Center at the University of Texas at Austin or obtained from Charles River Laboratories. Gerbils were housed in groups of up to 5 animals and maintained on a 12 h light/dark cycle.

ICC Neuron Targeting

We used an upstream domain (-2855 to +135) of the mouse calbindin-28 promoter (1) to target ICC CCK neurons. In transgenic mice, this regulatory domain had been reported to support expression in forebrain excitatory and inhibitory neurons. Among transgenic lines, variable expression was also in the colliculus, but specific cell types were not examined. We used nested PCR to remove restriction sites that interfered with downstream vector manipulations and added flanking Not1 and Sac1 sites to incorporate the promoter, which we termed CB3, into our existing AAV vectors (2). AAV:CB3-tdTomato was used to tag CCK neurons for in vitro studies (Figure 5).

In addition to promoters and genes, viral vectors contained the woodchuck post-transcriptional regulatory element (WPRE) and SV40 polyadenylation sequence and were flanked by two AAV inverted terminal repeats. Viruses were assembled using a modified helper-free system (Stratagene) as serotypes 2/1 (*rep/cap*). Viruses were purified on sequential cesium gradients according to published methods (3). Titers were measured using a payload-independent qPCR technique (4). Typical titers were $1x10^{10}$ genomes/microliter.

Stereotaxic Surgery

Mongolian gerbils of both sexes underwent stereotaxic surgery at 3-5 weeks of age for acute slice physiology and histology, and 9-12 weeks of age for *in vivo* recordings. Animals were anesthetized with isoflurane (2% in ~800 cc/minute O_2), placed on an infrared heating pad maintained at 37˚C, and secured with ear bars in a stereotaxic

frame (David Kopf Instruments, Tujunga, CA). For AAV expression, viruses were injected unilaterally or bilaterally into the ICC (from lambda: AP = –1.25 mm; ML = ±1.15 mm; DV = –3.2, –3.0, and –2.8 mm) using thin glass pipettes (10µm tip diameter) and Nanoject II injectors (Drummond Scientific). At each dorsal-ventral position, there were two injections of 9.2 nL each, spaced 2 minutes apart.

For *in vivo* electrophysiological recordings, 14 days after a virus injection a stainless steel head-post was affixed to the skull following previously described methods (5). UV curing dental cement was used to affix a custom-made stainless steel post above bregma and transcranial tungsten ground pin lateral to the post. The craniotomy above ICC was covered with bone wax and animal allowed to recover for *in vivo* recordings the next day. Otherwise, gerbils for acute slice physiology and histology were returned to their home cage for 10-14 days before *in situ* hybridization experiments, 14-20 days before electrophysiology experiments, and 14-25 days for anatomy or histology.

Histology

We used *in situ* hybridization to evaluate the specificity and coverage of virus-mediated reporter expression in CCK_E neurons. Analysis was performed using the RNAscope system (Advanced Cell Diagnostics). Whole brains were extracted without perfusion and flash-frozen in OCT medium (TissueTek) using a dry ice/ethanol bath. Brains were cryosectioned at 12µm (Leica CM3050S) and processed according to RNAscope instructions. Briefly, fixed and dehydrated sections were co-hybridized with proprietary probes (Advanced Cell Diagnostics) to neuronal marker transcripts, followed by differential fluorescence tagging. Cells identified using DAPI staining and fluorescence signals were co-localized on a Zeiss AxioZoom V16 microscope (Figure 1D). Sections of the ICC were probed for CCK, vesicular glutamate transporter 2 (VGluT2), glutamate decarboxylase 2 (GAD2), and tdTomato (Mm-CCK 402271, Mm-Slc17a6 319171, Mm-Slc32a1 319191, tdTomato 317041) with DAPI counterstain.

For immunohistochemical labeling, gerbils were deeply anesthetized with isoflurane and transcardially perfused with 5mL of 1% sodium nitrite in 0.1M phosphate-buffered saline (PBS), followed by 60mL of 4% paraformaldehyde (PFA) in 0.1M PBS. Brains were post-fixed overnight in 4% PFA at 4°C, removed from the skull, and

embedded in gelatin-albumin hardened with 5% glutaraldehyde and 37% PFA. Sections were cut at 35–65µm with a vibrating microtome (Leica VT1000S) and free-floating tissue was collected in PBS.

Free-floating tissue sections were washed in PBS. Tissue was permeabilized and nonspecific staining was blocked in a solution of 0.2% Triton X-100 and 5% normal goat serum in PBS for 1 hour. After blocking, tissue was treated with primary antibody in a solution containing 0.2% Triton X-100 and 5% normal goat serum in PBS overnight at 4°C Primary antibodies used were: guinea pig anti-VGluT2 (1:500, AB-2251-I, Millipore) and biotinylated goat anti-GFP (1:1000, ab6658, abcam). For fluorescent labeling, sections were incubated in a secondary antibody solution (1:200) containing 0.2% Triton X-100 and 5% normal goat serum for 2-3 hours. For biotinylated antibodies, tissue was incubated in an avidin-biotin solution (Vectastain Elite ABC HRP Kit, Vector Laboratories), and developed in a nickel-diaminobenzadine solution (DAB Peroxidase (HRP) Substrate Kit with Nickel, VectorLaboratories). Tissue sections were mounted on gelatin-coated slides and coverslipped (Vectashield Hardset Antifade Mounting Medium with DAPI for fluorescent tissue, Permount Mounting Medium for Ni-DAB reacted tissue).

Acute slice electrophysiology

Whole-cell recordings were conducted at 35°C using a Dagan BVC-700A amplifier (Dagan Corporation) in current-clamp mode with bridge balance and capacitance compensation. Data were low pass filtered at 5kHz, digitized at 50–100kHz, and acquired using custom algorithms in IgorPro (WaveMetrics). Neurons were visualized using a combination of fluorescence microscopy and either infrared differential interference contrast (IR-DIC) microscopy (Zeiss Axioskop 2FS Plus, Zeiss; IR-100 Infrared CCD monochrome video camera, Dage-MTI) or Dodt gradient contrast (Zeiss Examiner.D1; Zeiss Axiocam 503 mono). Glass recording electrodes (3–7MΩ) were filled with an intracellular solution containing 115mM K-gluconate, 4.42mM KCl, 0.5mM EGTA, 10mM HEPES, 10mM Na_2Phosphocreatine, 4mM MgATP, 0.3mM NaGTP, and 50µM Alexa 488 or Alexa 568, osmolality adjusted to 300mmol/kg with

sucrose, pH adjusted to 7.30 with KOH. All membrane potentials are corrected for a 10mV junction potential.

For cell-type specific fluorescence-targeted or photoactivation recordings, AAV:CB3-Flp and AAV:CaMKIIα-(ChR2-sfGFP)^{Flp} vectors were injected into the inferior colliculus to sensitize CCK_E neutrons to light. Full-field 470nm blue light from a custom LED system was presented through a 20X immersion objective (Zeiss). Onset, duration, and intensity of LEDs (Luxeon Star) were controlled by a dimmable LED driver (Buckpuck DC driver, Luxeon Star).

***In vivo* surgery and recordings**

Recordings were performed within a sound-attenuation chamber. Forty gerbils aged 11-14 weeks were anesthetized with an intraperitoneal injection of ketamine hydrochloride (90mg/kg) and xylazine (18mg/kg) before being secured to a custom-made head-post holder. Atropine sulfate (0.04mg/kg) was administered intramuscularly every 30-60 minutes as needed to reduce respiratory mucus secretions. Animals were maintained at 37˚C with a rectal probe feedback low-voltage DC electric heating pad (Harvard Apparatus). Bone wax was removed just prior to recording.

Glass-coated tungsten electrodes (2MΩ) or borosilicate glass electrodes (4-10MΩ) were used for single-unit recordings. Glass pipette were filled with an internal recording solution (0.05M Tris buffer, pH 7.4, and 0.15M KCl) and a silver wire. Electrodes were attached to a piezoelectric stereotaxic micropositioner (MP-285; Sutter Instruments) and registered to lambda and the skull surface before each penetration to ascertain recording location coordinates. For light stimulation, a multi-mode fiber optic (NA=0.39, 200μm core; Thorlabs Inc.) with a polished tip was coupled to an analog modulated blue DPSS laser (λ=473nm; Laserglow Technologies) was attached to a manually operated stereotax and independently lowered into the craniotomy at an angle of 15˚ off vertical. The tip of the fiber optic was slightly pressed into the tissue below the skull surface without distorting the IC surface located ~2.5mm below. The light power emitted from the tip of the fiber optic was measured at 20mW.

Stimulus delivery and neural recordings were controlled via custom-made MATLAB software. Acoustic stimuli were generated digitally by an RZ6 Multi I/O

Processor (Tucker-Davis Techonologies) and delivered by a calibrated closed-field speaker (ER2; Etymotic Research) with a 27cm wave guide and ear plug attachment. The ear plug was placed at the opening of the ear canal contralateral to the virally injected target ICC and sealed around the pinna with Vaseline. Care was taken not to allow for any air gaps or blockage of the ear plug. Under sealed conditions, the ER2 speakers have a flat speaker response at 80dB from 500Hz – 20kHz. Speaker calibration was completed using a 1/2" pressure field microphone (4192; Brüel & Kjaer). Neural signals were amplified and filtered (2400B Extracellular Preampflier; Dagan), before being digitized (RZ6) and sent to the custom software.

All sound stimuli were of 100ms duration and presented at 2/s or 4/s with a 5ms or 10ms rise/fall. Entry into the ICC was identified audio-visually by sound-evoked spikes to 65dB SPL broadband frozen white noise stimuli, and only neurons with a short latency (~10ms) were considered to be ICC. The stimulus was then turned off, and light pulses of 10-50ms duration were presented at 2/s as search stimuli for the virus injection site. The frequency response area (FRA) of light sensitive and insensitive units were characterized by presenting pseudorandom sinusoidal tone and intensity level combinations repeated 10 times for each. Tones were given over a range of 2-4 octaves in steps of $1/8^{th}$ octave, and intensity was varied in steps of 10dB SPL. Light sensitivity for relevant units was reconfirmed after obtaining an FRA. Following the last recording in a session, an electrolytic lesion was made with a tungsten electrode by passing 0.8µA DC for 15 seconds via a high-voltage constant current source (Digital Midgard Precision Current Source; Stoelting). If using a glass electrode, it was replaced with a tungsten electrode, registered to lambda, and brought to the same coordinates as the last recording site. The metal electrode was retracted after 5 minutes and the animal was transcardially perfused with 5mL of 1% sodium nitrite in 0.1M PBS, followed by 60mL of 4% PFA in 0.1M PBS and prepared for histological processing. Recording sites for CCK_E neurons (marked with electrolytic lesions) covered the following relative positions within the ICC: caudal to rostral = 32-82%, medial to lateral = 10.3-57%, dorsal to ventral = 14.6-53.7%.

Analysis

All data were analyzed using custom algorithms in IgorPro (WaveMetrics) or Matlab (Mathworks).

In vitro, the degree of spike frequency adaptation (adaptation ratio, AR) was calculated using the average interspike interval (ISI) for the first and last five APs in a 500ms current injection:

$$(\mathrm{AR} = \frac{\sum_{n-3}^{n} \mathrm{ISI}}{4} / \frac{\sum_{1}^{4} \mathrm{ISI}}{4}).$$

ARs were calculated for firing rates in four bins between 20 and 100Hz. Instantaneous firing rate was defined as the maximal firing rate of the first four APs in response to the maximal current injection that produced vigorous firing. AP threshold was defined as the membrane potential at which the second derivative of membrane potential crossed $500\mathrm{mV/ms^2}$. AP height was defined as the voltage difference between the AP threshold and peak AP voltage, and AP half-width was defined as the duration of the AP at half the maximal AP height. Steady state input resistance calculated from a linear fit of the current-voltage relationship for hyperpolarizing current injections that correspond to voltage changes between 0 and -15mV from rest. Time constant was calculated from an exponential fit of 20-40 repetitions of hyperpolarizing current injections that correspond to a -5mV voltage change. Sag ratios were calculated as the ratio between the peak voltage change and steady state voltage change in response to a hyperpolarizing current injection where the minimum voltage was approximately -80mV.

Since cells in the ICC are intrinsically connected and the CCK_E population is excitatory, we used conservative criteria to select units that were "direct" recordings from CCK_E neurons. Direct recordings were defined as those from CCK_E neurons expressing ChR2. "Indirect" recordings were defined as those from cells receiving excitatory input from a CCK_E neuron expressing ChR2 strong enough to evoke an action potential in the postsynaptic cell. "Direct" recordings of CCK_E neurons met two criteria: relatively low jitter (≤ 6ms) and burst firing, as quantified by instantaneous firing rate >120 spikes/s. Units not meeting both criteria were deemed "indirect" and excluded from analysis. To aid in our criteria selection, we preformed light intensity tests on neurons with robust responses to light at the highest light power (SI Appendix, Figure S3G-H). As light intensity was reduced, first spike latency and jitter increased while spike rate often decreased. However, the *in vivo* bursting pattern seen during robust light responses

remained present at all light powers for that unit. Consequently, instantaneous firing rate became an important criterion for unit classification. Despite the consistency in the burst pattern in apparent direct responses, we wanted to be cautiously exclusive of units that might have been "indirect" at the risk of excluding some "direct" units with weak ChR2 activation. A burst criterion of 120 spikes/s (instantaneous firing rate of the first 3 light evoked spikes) provided the best separation of CCK_E units from the broader population of non-ChR2 infected ICC units that would be necessarily activated only by local synapses (SI Appendix, Figure S3D). Slice recordings from CCK_E neurons provide further context for the robust firing observed during direct recordings from CCK_E neurons *in vivo* (SI Appendix, Figure S2E), as well as the bursting behavior following light presentations (SI Appendix, Figure S2F). Single unit recordings were verified *post hoc* via manual thresholding and spike morphology (Figure 6A).

The sharpness of spectral tuning *in vivo* was calculated by measuring Q-values from each FRA. First each FRA was reduced to a tuning curve defined by setting a spike threshold for each frequency presented. Spike threshold was set as the lowest sound intensity needed to trigger at least one spike 50% of the time during a sound stimulus. The Q-value was then determined by dividing the middle frequency for a given sound intensity in the tuning curve, by the bandwidth of the FRA tuning curve at that intensity value. Best frequency was defined as the frequency that elicited the maximum firing for that neuron.

Significant differences were measured with ANOVA tests and a Tukey's post hoc analysis, where appropriate. Statistical significance was defined as $p<0.05$. Data are expressed as mean±SEM unless otherwise noted.

References

1. O. Pavlou, R. Ehlenfeldt, S. Horn, H. T. Orr, Isolation, characterization and in vivo analysis of the murine calbindin-D28K upstream regulatory region. *Brain Res Mol Brain Res* **36**, 268-279 (1996).
2. P. Mehta *et al.*, Functional Access to Neuron Subclasses in Rodent and Primate Forebrain. *Cell Rep* **26**, 2818-2832 e2818 (2019).

3. J. C. Grieger, S. Snowdy, R. J. Samulski, Separate basic region motifs within the adeno-associated virus capsid proteins are essential for infectivity and assembly. *J Virol* **80**, 5199-5210 (2006).
4. C. Aurnhammer *et al.*, Universal real-time PCR for the detection and quantification of adeno-associated virus serotype 2-derived inverted terminal repeat sequences. *Hum Gene Ther Methods* **23**, 18-28 (2012).
5. M. A. Muniak, Z. M. Mayko, D. K. Ryugo, C. V. Portfors, Preparation of an awake mouse for recording neural responses and injecting tracers. *J Vis Exp* 10.3791/3755 (2012).

Supplementary Data

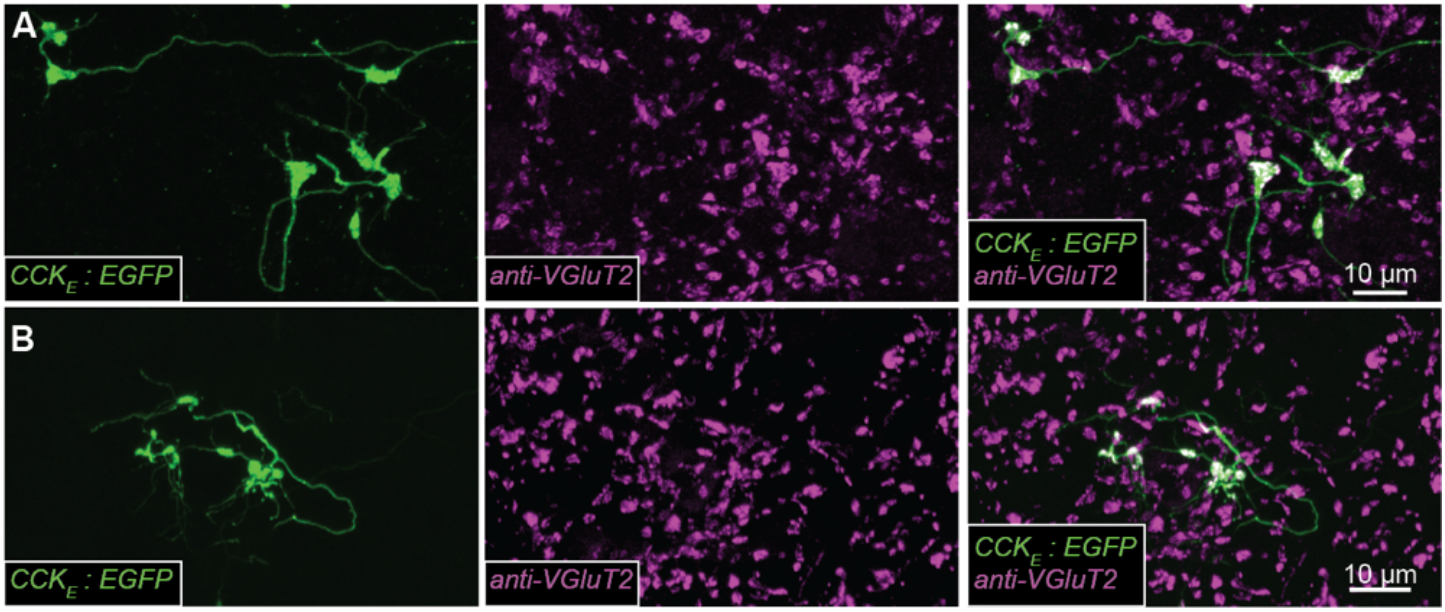

Supplemental Figure 1. CCK_E projections in the vMGB have large, VGluT2+ synaptic boutons. **(A-B)** Maximum projections showing viral-mediated EGFP expression (green) in CCK_E neurons immunostained for VGluT2 (magenta).

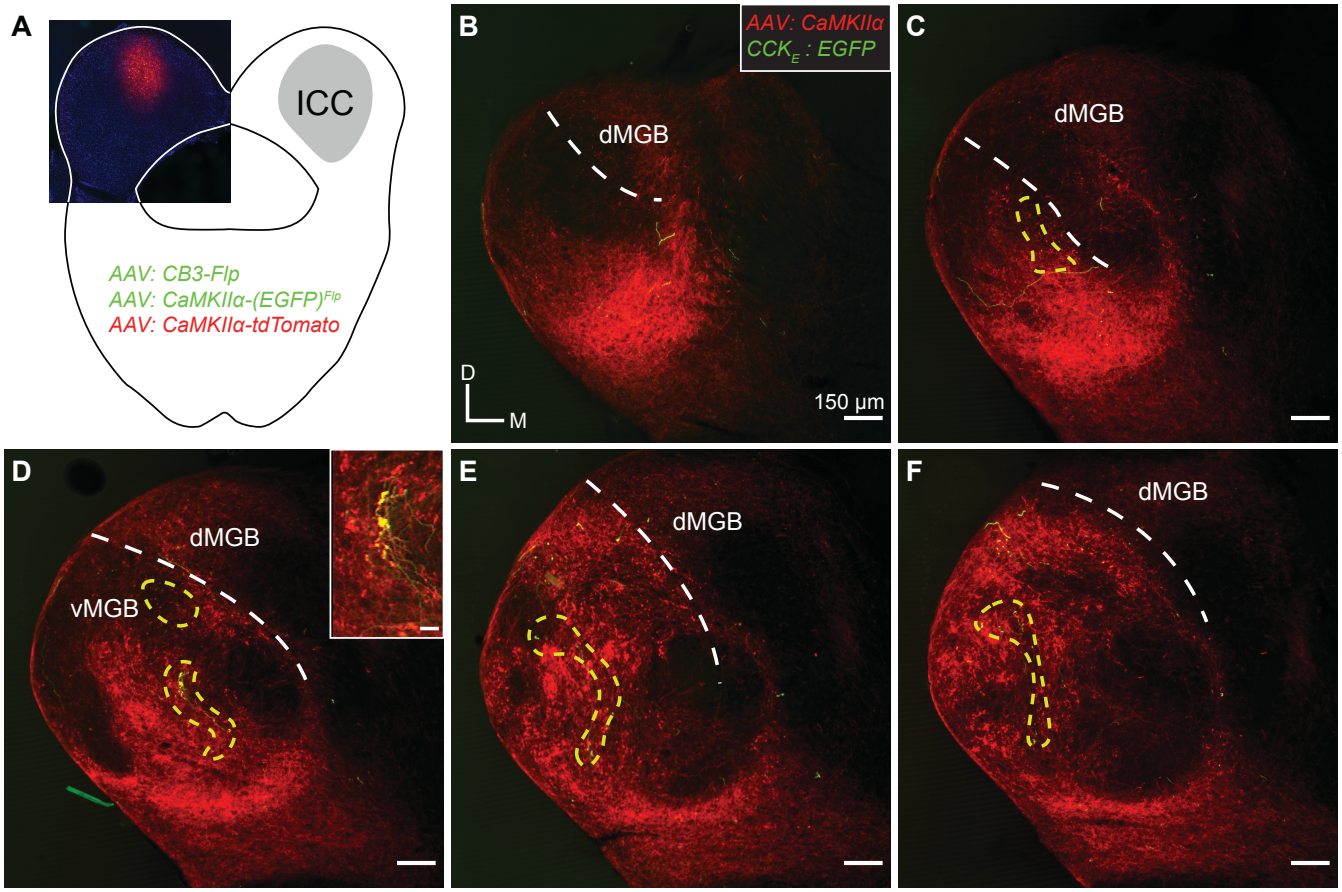

Supplemental Figure 2. Axons from CCK_E neurons are more spatially restricted in the vMGB than axons from excitatory ICC neurons.
(A) A mixture of AAVs was stereotaxically injected into the ICC to express EGFP in CCK_E neurons and tdTomato in excitatory neurons. Unilateral ICC injection site (red) is shown in a representative 30µm thick coronal section.
(B-F) Representative 30µm alternating coronal sections from the unilateral injection in A. Serial sections are spaced 60µm apart. Axons from excitatory neurons (red) spread broadly and tonotopically within the vMGB. Axons from CCK_E neurons (green) have a more restricted targeting, despite being such a large portion of the excitatory population (see Figure 1A). Yellow dotted lines surround areas with CCK_E terminal endings. Inset in D features terminal morphology at higher power (inset scale bar: 25µm).

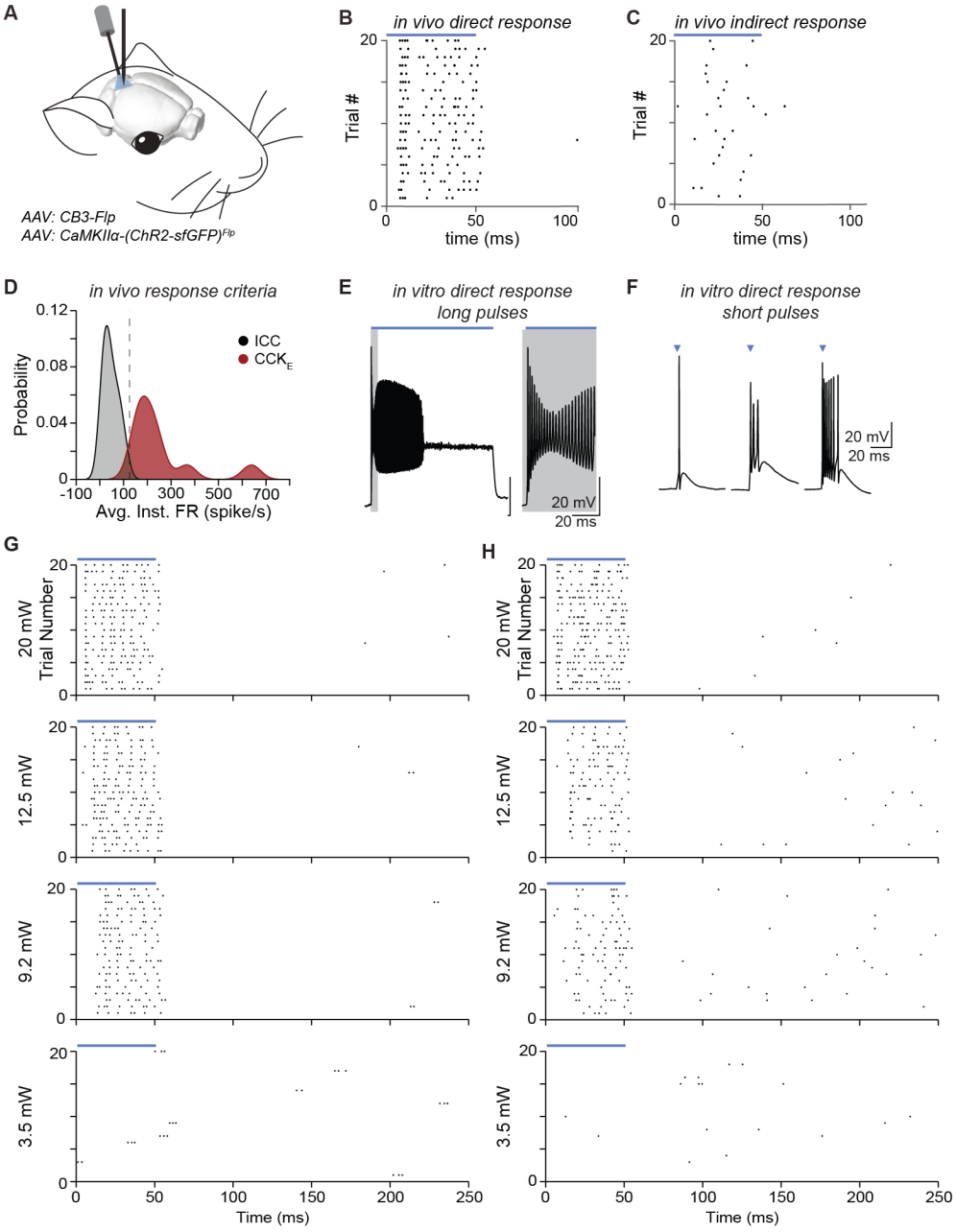

Supplemental Figure 3. CCK_E neurons can be targeted for recordings *in vivo* using optogenetics.

(A) Experimental preparation for in vivo recording of ICC CCK_E neuron responses to auditory stimuli. ChR2 was expressed in CCK_E neurons. The recording electrode was positioned vertically to approach the ICC; the optic fiber for light stimulation was independently positioned at 15˚rostral to vertical.

(B-C) Example raster plots of the responses of two cells to 20 presentations of 50ms blue light. Responses in B were direct recordings from a CCK_E neuron identified based on the low jitter of the first spike, the presence of short bursts of 2-4 spikes, and persistent firing over the duration of the light presentation. Responses in C were of a cell that did not express ChR2. Spikes were sparse with a high first spike jitter.

(D) The criteria for categorizing light response type as a direct CCK_E recording (red) or a recording from an ICC neuron indirectly stimulated by light (grey) was primarily based upon the instantaneous firing rate of the first 3 light evoked spikes. We analyzed CCK_E neurons with light-evoked instantaneous firing rates above 120 spikes/s.

(E) Light-evoked action potential bursting can be observed in CCK_E neurons recorded intracellularly with patch-clamp recordings *in vitro*. Example *in vitro* trace from a CCK_E neuron expressing ChR2. Long (1000ms) pulses of blue light, analogous to longer light presentations *in vivo*, evokes a train of spikes. Grey inset shows 50ms of activation from the example trace in which spikes occur throughout the light presentation, with some spike height accommodation.

(F) Example traces from CCK_E neurons expressing ChR2. Short (2ms) pulses of blue light (blue triangles) reliably evoked bursts of action potentials in CCK_E neurons, similar to bursting seen *in vivo*.

(G-H) Example raster plots of the responses of two cells to 20 presentations of 50ms blue light at different intensities.